Should Contemporary Density Functional Theory Methods Be Used to Study the Thermodynamics of Radical Reactions?

Ekaterina I. Izgorodina,[†] David R. B. Brittain, Jennifer L. Hodgson, Elizabeth H. Krenske, Ching Yeh Lin, Mansoor Namazian, and Michelle L. Coote*

ARC Centre of Excellence in Free-Radical Chemistry and Biotechnology, Research School of Chemistry, Australian National University, Canberra ACT 0200, Australia

Received: July 24, 2007

The performance of a variety of DFT functionals (BLYP, PBE, B3LYP, B3P86, KMLYP, B1B95, MPWPW91, MPW1B95, BB1K, MPW1K, MPWB1K, and BMK), together with the ab initio methods RHF, RMP2, and G3(MP2)-RAD, and with ONIOM methods based on combinations of these procedures, is examined for calculating the enthalpies of a range of radical reactions. The systems studied include the bond dissociation energies (BDEs) of R−X (R = CH_3, CH_2F, CH_2OH, CH_2CN, CH_2Ph, $CH(CH_3)Ph$, $C(CH_3)_2Ph$; X = H, CH_3, OCH_3, OH, F), RCH(Ph)−X (R = CH_3, CH_3CH_2, $CH(CH_3)_2$, $C(CH_3)_3$, CH_2F, CH_2OH, CH2CN; X = H, F), R−TEMPO (R = CH_3, CH_2CH_3, $CH(CH_3)_2$, $C(CH_3)_3$, $CH_2CH_2CH_3$, CH_2F, CH_2OH, CH_2CN, $CH(CN)CH_3$, $CH(Cl)CH_3$; TEMPO = 2,2,6,6,-tetramethylpiperidin-1-yloxyl) and HM_1M_2−X (M_1, M_2 = $CH_2CH(CH_3)$, $CH_2CH(COOCH_3)$, $CH_2C(CH_3)(COOCH_3)$; X = Cl, Br), the β-scission energies of $RXCH_2^{\bullet}$ and $RCH_2CHPh^{\bullet}$ (R = CH_3, CH_2CH_3, $CH(CH_3)_2$, $C(CH_3)_3$; X = O, S, CH_2), and the enthalpies of several radical addition, ring-opening, and hydrogen- and chlorine-transfer reactions. All of the DFT methods examined failed to provide an accurate description of the energetics of the radical reactions when compared with benchmark G3(MP2)-RAD values, with all methods tested showing unpredictable deviations of up to 40 kJ mol^{-1} or more in some cases. RMP2 also shows large deviations from G3(MP2)-RAD in the absolute values of the enthalpies of some types of reaction and, although it fares somewhat better than the DFT methods in modeling the relative values, it fails for substituents capable of strongly interacting with the unpaired electron. However, it is possible to obtain cost-effective accurate calculations for radical reactions using ONIOM-based procedures in which a high-level method, such as G3(MP2)-RAD, is only used to model the core reaction (which should contain all substituents α to the reaction center), and the full system is modeled using a lower-cost procedure such as RMP2.

Introduction

Radical reactions are ubiquitous in many biological processes, in atmospheric chemistry, and in several important industrial processes including polymerization and combustion. They are often highly reactive and participate in multistep chain processes, features that can hamper experimental determinations of their rate and equilibrium constants. Computational methods are thus an attractive option for studying radical chemistry and are already proving to be extremely useful tools in kinetic modeling and reagent design.[1] However, their success depends upon the availability of accurate low-cost methods for studying radical reactions such as addition, abstraction, homolysis, and ring opening.

Owing to its relatively low computational expense, density functional theory (DFT) methods are most frequently adopted for studying radical reactions, particularly for larger chemical problems such as polymerization. However, despite their widespread use, a small but growing number of studies have indicated that the approximate exchange-correlation functionals that are currently in use can be subject to considerable error. For example, we have shown that a wide range of pure and hybrid DFT methods fail even to reproduce the correct qualitative trends in simple R−X bond-dissociation reactions (R = Me, Et, *i*-Pr, *t*-Bu; X = H, CH_3, OCH_3, OH, F).[2] We have also shown that popular DFT methods such as B3LYP have significant errors (as much as 50 kJ mol^{-1}) when used to calculate the enthalpies of some radical addition reactions.[3,4] Perhaps of even greater concern has been the recent demonstrations that contemporary DFT methods fail even in simple closed-shell systems, such as the cyclization energies of alkenes and alkane isomerization energies, and show large errors in the bond separation energies of a large range of organic compounds and in the heats of formation of larger molecules.[5] These results would tend to suggest that the problems with contemporary DFT methods could be quite widespread.

In the light of these recent studies and the growing use of DFT methods for computational thermochemistry, it is important to investigate their suitability for studying radical reactions and, if necessary, identify low-cost alternative methods. To this end, in the present work we examine the accuracy of various DFT methods, together with that of ab initio molecular orbital theory methods such as RMP2 and G3(MP2)-RAD, for studying the thermodynamics of a range of radical reactions including hydrogen and halogen atom abstraction, radical addition to various types of double bonds, homolysis and radical ring-opening, both in representative prototypical systems, and a

* Corresponding author. E-mail: mcoote@rsc.anu.edu.au. Fax: 61 2 6125 0750.

[†] Current address: School of Chemistry, Monash University, Victoria 3800, Australia.

10.1021/jp075837w CCC: $37.00
Published on Web 09/22/2007

number of practical case studies involving larger molecules. On the basis of these results, we determine whether or not DFT should be used to study the thermodynamics of radical reactions and identify suitable low-cost alternative methods.

Theoretical Procedures

Standard ab initio molecular orbital theory and density functional theory (DFT) calculations were carried out by using the GAUSSIAN 03[6] and MOLPRO 2002.3[7] programs. Reaction enthalpies (0 K) were calculated for a wide variety of radical reactions with a view to examining the effect of ab initio and density functional theory on the accuracy of the results. To allow for a consistent comparison between the various methods, all geometries were optimized with B3LYP/6-31G(d), and frequency calculations were also carried out at this level to ensure convergence to a local minimum had been achieved. All zero-point vibrational energies and thermochemical corrections were calculated using scaled[8] B3LYP/6-31G(d) frequencies.

Improved energies were calculated by using a range of methods including HF, MP2, a variety of DFT methods, and the high-level composite procedure G3(MP2)-RAD.[9] Because we were unable to find the G3MP2 large basis set of this latter procedure for Br in GAUSSIAN, MOLPRO, or the EMSL Gaussian basis set order form, a modified G3(MP2)-RAD procedure was used for the BDE data in Table 6.[10] In this procedure, calculations with the double- and triple-ζ Pople basis sets were replaced with calculations using the respective double- and triple-ζ Dunning basis sets, cc-pVDZ and cc-pVTZ. All RHF, DFT, and RMP2 single-point calculations were performed using the 6-311+G(3df,2p) basis set unless noted otherwise. All DFT single-point calculations were performed using the ultrafine grid of GAUSSIAN.

Throughout the work, all DFT calculations were carried out using unrestricted wave functions, whereas calculations at the HF, MP2, and CCSD(T) level of theory used restricted (or restricted open-shell) wave functions, as denoted with an "R" prefix. Assessment studies of prototypical radical reactions have indicated that restricted-open-shell methods outperform unrestricted methods for ab initio methods such as MP2.[11] In contrast, DFT methods appear to be much less sensitive,[12] and we have therefore opted for unrestricted DFT because restricted-open-shell DFT is logically infeasible.[13]

As in our previous study of the homolytic R−X BDEs,[2] a variety of different functionals were considered. These include the traditional pure functionals, BLYP[14] and PBE,[15] the widely used hybrid three-parameter functionals, B3LYP[16] and B3P86,[16,17] and a number of relatively new functionals, including KMLYP,[18] B1B95,[19] MPWPW91,[20] MPW1B95,[21] BB1K,[22] MPW1K,[23] MPWB1K,[21] and BMK.[24] These latter functionals have been specifically optimized to give improved performance for studying the thermodynamics and/or kinetics of chemical reactions. With the exception of BMK, the new DFT functionals consist of modified original exchange (such as Becke88, Slater, Perdew−Wang) and correlation (such as Becke95, LYP, PW91, VWN) functionals. With the exception of BLYP and PBE, all of the DFT functionals include a portion of the exact HF exchange, which varies from 20% for B3LYP to 55.7% for KMLYP. The BMK functional is somewhat different to the others, as it simulates a variable exact exchange. This is achieved by the combination of exact exchange (42%) and terms depending on the kinetic energy density. The KMLYP functional differs from the other DFT methods in that it contains an additional higher-level correction (HLC) term based on the number of unpaired electrons (n_r) and the number of lone pair electrons (n_p): HLC $= -ln_r - mn_p$, where $l = 0.00258$ hartree and $m = 0.01053$ hartree for atoms and 0.01231 hartree for molecules. This HLC makes a significant contribution to the absolute values of the BDEs studied in the present work but cancels entirely from the relative values, and from the other reaction energies studied herein.[25]

During the course of the work, we also designed and tested a series of ONIOM-based procedures. In the ONIOM method of Morokuma and co-workers,[26] one first defines a "core" section of the reaction that typically includes all forming and breaking bonds and the principal substituents attached to them. In forming the core system, deleted substituents are replaced with "link atoms" (typically hydrogens), chosen so that core system provides a good chemical model of the reaction center. The core system is studied at both a high level of theory and also a lower level, while the full system is studied only at the lower level of theory. The high-level energy for the full system is then approximated as the sum of the high-level energy for the core system and the substituent effect, as measured at the lower level of theory. This approximation is valid provided that the low level of theory measures the substituent effect accurately; this in turn depends not only the level of theory chosen but also the manner in which the core is defined. In the present work, we explore the performance of ONIOM for various combinations of core sizes and levels of theory.

It should be noted that the ONIOM method is normally used as a QM/MM approach to studying larger biological reactions and is normally applied to the calculation of geometries and frequencies as well as energies.[26] This differs from the present work in that we use a QM/QM version of ONIOM and only apply the method to the calculation of single point energies. That is, the geometries of the core and full systems are both fully optimized at the same level of theory used in the rest of the calculations presented herein, B3LYP/6-31G(d). Under these conditions, the ONIOM technique is equivalent to approximating the enthalpy of the chemical reaction as a linear combination of the enthalpy for the core reaction (as measured at a high level of theory) and the relative values of the core and full reactions (as measured at a lower level of theory). This type of technique is also sometimes referred to as an "isodesmic method", particularly when applied using experimental values for the core reaction and computational values only for the substituent effect.

Results and Discussion

Theoretical Design. Previously, we have shown that contemporary DFT methods fail to reproduce the effect of increasing alkylation (R = Me, Et, *i*-Pr, *t*-Bu) on the relative values of R−X bond dissociation energies for X = H, CH_3 OCH_3, OH, and F.[2] At the same time, these trends were modeled correctly (when compared with experiment) by high-level composite methods such as G3(MP2)-RAD and G3-RAD and also the lower-cost method RMP2/6-311+G(3df,2p). In chemical terms, this implies that the DFT methods studied fail to model correctly the thermodynamics of chain-transfer reactions such as hydrogen, hydroxyl and halogen atom abstractions, and the stabilization energies of radicals.

To investigate the generality of these results, we have now expanded our studies of homolytic R−X BDEs to include other R-groups (R = CH_2F, CH_2OH, CH_2CN, benzyl, 1-phenylethyl, and cumyl; X = H, CH_3 OCH_3, OH, and F) covering a wider range of electronic properties (Table 1). We have also tested the performance of the various low-cost methods for a second major class of radical reactions, β-scissions of the form

TABLE 1: R−X Bond Dissociation Energies (0 K, kJ mol^{-1})[a] for R = CH_3, CH_2F, CH_2OH, CH_2CN, CH_2Ph, $CH(CH_3)Ph$, and $C(CH_3)_2Ph$, and X = H, CH_3, OCH_3, OH, and F

X−R	RHF	PBE	BLYP	B3LYP	B3P86	KMLYP	B1B95	MPWPW91	MPW1B95	BB1K	MPW1K	MPWB1K	BMK	RMP2	G3(MP2)-RAD	expt
H−CH_3	328.8	421.0	420.1	424.6	435.6	430.9	429.7	418.7	431.4	429.1	414.7	430.5	431.0	417.4	428.4	430.0 ± 0.4
H−CH_2F	323.5	397.9	399.3	406.9	416.7	414.9	409.1	396.7	411.1	410.6	399.2	412.2	413.9	404.4	416.0	416.3 ± 4.2
H−CH_2OH	307.6	376.2	376.9	385.3	395.6	394.0	386.9	375.1	389.0	389.1	379.6	390.7	391.2	385.1	396.8	395.92 ± .63
H−CH_2CN	323.5	373.0	370.3	380.4	392.4	392.7	385.9	371.3	388.1	388.5	377.2	390.2	394.3	386.2	396.5	387.7
H−CH_2Ph	302.7	350.9	347.5	357.3	369.5	366.3	362.3	349.3	364.5	364.4	353.0	365.9	368.2	367.0	369.4	363.1 ± 6.3
H−$CH(CH_3)Ph$	293.6	334.5	333.2	343.6	354.3	352.4	346.6	333.3	348.9	349.5	339.6	351.2	355.4	357.7	360.2	348.3 ± 6.3
H−$C(CH_3)_2Ph$	290.9	326.0	326.4	337.4	346.8	346.5	338.6	325.0	341.1	342.2	333.6	344.0	350.2	355.1	358.2	338.3 ± 4.2
CH_3−CH_3	257.9	364.9	337.9	343.2	360.9	368.4	369.0	355.7	373.8	368.3	348.2	372.2	370.1	371.3	361.0	367.7 ± 0.8
CH_3−CH_2F	277.8	369.5	344.0	352.4	368.9	381.0	375.1	360.7	380.7	376.5	359.3	381.1	379.4	386.4	376.1	382.6 ± 8.4
CH_3−CH_2OH	257.5	343.0	316.5	325.9	343.2	356.0	348.4	334.1	354.1	350.6	335.3	355.2	353.0	365.0	354.7	353.2 ± 4.2
CH_3−CH_2CN	259.6	324.1	294.8	305.9	324.8	338.0	332.1	315.1	337.7	334.7	317.8	339.2	341.6	352.1	339.5	333.2 ± 12.6
CH_3−CH_2Ph	237.0	302.2	270.9	282.0	301.7	312.5	308.4	292.9	314.2	310.7	293.6	315.2	315.9	338.0	315.5	313.3 ± 7.1
CH_3−$CH(CH_3)Ph$	227.1	288.3	256.9	269.3	288.9	303.1	296.1	278.6	302.7	299.4	282.5	304.6	306.6	335.6	312.5	304.6 ± 6.3
CH_3−$C(CH_3)_2Ph$	215.0	274.7	241.9	256.1	276.5	295.1	284.5	264.2	292.1	289.1	271.6	295.1	298.4	334.4	311.0	294.6 ± 8.4
CH_3O−CH_3	211.0	329.9	304.1	310.3	329.0	335.9	330.8	321.6	336.3	328.9	311.1	333.4	336.4	370.3	340.3	340.8 ± 4.2
CH_3O−CH_2F	261.3	366.9	340.2	349.9	368.9	381.2	369.0	358.6	375.5	369.5	354.5	374.7	378.4	419.4	388.1	
CH_3O−CH_2OH	244.5	344.0	316.5	327.3	347.1	360.2	346.2	335.8	352.8	347.5	334.2	352.7	355.6	401.1	370.3	
CH_3O−CH_2CN	200.9	280.8	252.6	263.5	283.5	294.6	284.4	272.6	290.8	285.3	270.2	290.3	298.1	342.5	311.1	
CH_3O−CH_2Ph	197.1	274.3	244.6	256.7	277.2	297.6	278.3	265.9	284.9	279.4	263.7	284.5	288.8	341.1	301.5	
CH_3O−$CH(CH_3)Ph$	182.7	260.4	228.6	242.4	264.3	288.6	266.2	251.1	274.0	268.4	251.7	274.5	280.0	342.1	301.8	
CH_3O−$C(CH_3)_2Ph$	185.8	258.1	227.3	242.5	263.5	292.1	265.2	248.5	273.7	268.6	252.5	275.1	282.6	349.2	308.3	
HO−CH_3	236.5	386.9	360.9	358.5	377.8	374.9	379.3	378.5	383.2	372.4	351.8	375.9	380.3	396.9	370.6	376.74 ± 0.71
HO−CH_2F	289.2	427.4	399.8	400.7	420.8	423.4	420.4	418.8	425.3	416.0	398.3	420.1	425.0	448.1	420.3	
HO−CH_2OH	274.7	406.5	378.7	380.4	400.8	404.1	399.4	398.1	404.4	395.7	379.8	399.9	404.0	431.1	403.9	
HO−CH_2CN	227.2	339.0	310.6	312.6	333.1	334.1	333.6	330.7	338.2	329.4	311.8	333.3	341.7	366.8	339.7	
HO−CH_2Ph	222.3	331.2	301.3	304.7	325.8	336.4	326.3	322.7	331.4	322.5	304.1	326.7	332.4	365.4	329.9	337.4 ± 7.5
HO−$CH(CH_3)Ph$	231.6	335.9	306.2	310.7	331.3	345.0	331.5	327.2	337.2	328.6	311.3	333.3	340.9	380.5	344.1	
HO−$C(CH_3)_2Ph$	231.5	331.5	302.2	308.2	328.2	346.1	328.4	322.3	334.9	326.6	309.7	332.0	341.2	386.0	349.4	
F−CH_3	297.6	477.0	457.7	447.4	463.0	477.9	462.2	470.1	465.2	450.0	426.2	452.9	462.6	476.2	452.5	451.0 ± 8.4
F−CH_2F	342.0	508.8	486.8	480.1	497.4	517.8	494.8	501.5	498.6	485.1	464.5	488.6	498.4	519.5	493.7	485.8 ± 8.8
F−CH_2OH	334.4	495.9	474.2	467.9	485.0	505.5	481.2	488.9	485.2	472.0	453.1	475.6	484.6	508.1	483.0	
F−CH_2CN	274.0	417.5	396.3	389.5	405.8	423.3	404.0	410.7	407.5	393.9	372.9	397.1	410.0	433.2	408.6	
F−CH_2Ph	286.1	424.3	401.6	396.6	413.5	432.1	411.9	417.4	416.0	402.5	380.9	406.1	416.4	443.2	411.1	402.4 ± 8.4
F−$CH(CH_3)Ph$	297.4	430.0	408.5	404.6	420.1	441.8	418.0	422.9	422.7	409.4	389.0	413.5	425.3	457.3	424.8	
F−$C(CH_3)_2Ph$	309.0	436.0	415.7	412.9	427.3	452.6	424.9	428.7	430.2	417.4	397.8	421.9	435.2	471.2	439.0	
								Absolute Values								
mean abs dev	110.0	17.2	32.8	27.1	11.9	8.8	12.0	20.6	9.1	12.5	28.4	9.4	6.3	23.5	0	
max dev.	154.9	50.2	81.0	65.8	44.8	25.4	43.1	59.8	34.6	39.7	55.8	33.2	25.7	40.9	0	
								Relative Values[b]								
mean abs dev	16.6	18.9	21.1	15.6	14.8	7.4	16.2	18.9	15.0	12.9	9.6	12.1	9.8	5.5	0	
max dev	33.0	40.2	46.0	37.1	34.4	23.3	34.5	41.5	31.7	29.2	26.6	27.1	21.8	13.1	0	

[a] All calculations were performed using B3LYP/6-31G(d) optimized geometries and incorporate scaled B3LYP/6-31G(d) zero-point energy corrections. All single-point energy calculations except those at the G3(MP2)-RAD level were performed using the 6-311+G(3df,2p) basis set. The R = CH_3 data were drawn largely from ref 2 and is included as the reference system, though some additional levels of theory were calculated for present work. The experimental data were taken from ref 31 and corrected to 0 K using temperature corrections calculated at the B3LYP/6-31G(d) level. [b] The relative value of the reaction enthalpy was calculated as the difference between it and the corresponding value for R = CH_3. In calculating the MADs of the relative values, the R = CH_3 data were omitted as their MADs are equal to zero by definition.

TABLE 2: Enthalpies (0 K, kJ mol^{-1})[a] of the β-scission Reactions, R−$XCH_2^\bullet$ → $R^\bullet$ + X=CH_2 and R−$CH_2CHPh^\bullet$ → $R^\bullet$ + CH_2=CHPh, for R = CH_3, CH_2CH_3, $CH(CH_3)_2$, and $C(CH_3)_3$ and X = CH_2, O, and S

R−X	RHF	PBE	BLYP	B3LYP	B3P86	KMLYP	B1B95	MPWPW91	MPW1B95	BB1K	MPW1K	MPWB1K	BMK	RMP2	G3(MP2)-RAD	expt
$CH_3-CH_2CH_2^\bullet$	68.4	99.4	65.4	79.2	101.6	126.3	93.0	92.4	98.9	99.9	110.6	104.8	99.2	97.1	85.9	93.4
$CH_2CH_3-CH_2CH_2^\bullet$	65.7	86.8	51.5	67.8	90.5	118.9	81.6	79.3	88.2	90.2	101.9	95.4	91.6	98.4	85.4	88.8
$CH(CH_3)_2-CH_2CH_2^\bullet$	53.6	72.7	35.6	52.0	78.2	110.8	69.4	64.5	77.0	79.4	91.5	85.4	83.5	99.6	84.1	
$C(CH_3)_3-CH_2CH_2^\bullet$	43.9	57.4	17.9	38.3	63.7	100.0	55.5	48.5	64.4	67.0	77.7	73.7	74.0	99.4	81.9	
$CH_3-OCH_2^\bullet$	2.2	41.3	15.2	25.6	43.1	70.2	37.1	34.2	43.5	42.2	45.9	47.3	36.8	24.6	22.5	24.1
$CH_2CH_3-OCH_2^\bullet$	13.6	42.0	15.5	28.3	45.5	76.6	39.1	34.6	46.3	45.7	50.7	51.4	42.1	38.2	34.9	42.3
$CH(CH_3)_2-OCH_2^\bullet$	15.0	37.8	9.8	24.7	42.8	77.8	36.3	29.8	44.3	44.2	49.3	50.5	43.1	46.7	42.0	
$C(CH_3)_3-OCH_2^\bullet$	5.3	24.6	−5.3	11.9	31.4	70.6	25.6	15.9	34.5	34.7	38.9	41.7	35.9	46.8	41.2	
$CH_3-SCH_2^\bullet$	87.8	138.5	105.9	116.0	137.3	159.7	132.0	130.7	137.5	136.7	141.8	141.2	133.5	120.2	111.7	122.8
$CH_2CH_3-SCH_2^\bullet$	85.5	128.2	93.8	106.2	128.3	154.1	122.7	119.9	129.1	128.9	134.9	134.0	128.5	125.6	114.1	
$CH(CH_3)_2-SCH_2^\bullet$	79.4	116.8	80.7	95.0	118.0	147.1	112.5	107.9	119.6	119.8	126.2	125.5	122.0	129.2	114.9	
$C(CH_3)_3-SCH_2^\bullet$	66.6	102.7	64.0	80.1	105.0	137.7	100.3	92.9	108.4	108.7	114.0	115.1	113.6	130.5	113.6	
$CH_3-CH(Ph)CH_2^\bullet$	78.3	138.0	104.9	116.7	138.6	165.7	132.4	129.9	138.4	138.7	146.5	143.5	137.0	127.5	125.9	
$CH_2CH_3-CH(Ph)CH_2^\bullet$	75.9	125.3	91.1	105.4	127.6	158.6	121.0	116.8	127.9	128.9	138.1	134.4	129.7	129.4	126.0	
$CH(CH_3)_2-CH(Ph)CH_2^\bullet$	62.5	110.9	74.3	90.5	114.0	148.7	107.2	101.7	115.1	116.3	125.9	122.5	119.8	131.8	125.1	
$C(CH_3)_3-CH(Ph)CH_2^\bullet$	49.3	95.0	55.2	73.9	99.4	139.1	94.1	84.5	103.4	104.7	112.7	112.0	110.9	134.5	124.8	
								Absolute Values								
mean abs dev	36.3	13.0	34.9	21.1	11.8	27.9	12.3	15.3	11.2	10.8	13.1	12.0	8.3	9.1	0	
max dev	75.5	29.8	69.7	51.0	25.6	48.0	30.7	40.4	25.9	25.1	30.2	29.5	21.9	17.5	0	
								Relative Values[b]								
mean abs dev	12.0	25.1	28.3	24.0	22.3	14.6	22.4	26.3	20.6	19.5	18.6	18.2	14.6	4.3	0	
max dev	27.9	41.9	48.6	41.7	38.1	25.5	37.2	44.3	33.9	32.9	32.7	30.4	25.0	8.4	0	

[a] All calculations were performed using B3LYP/6-31G(d) optimized geometries and incorporate scaled B3LYP/6-31G(d) zero-point energy corrections. All single-point energy calculations except those at the G3(MP2)-RAD level were performed using the 6-311+G(3df,2p) basis set. Seven of the reactions ($^\bullet CH_3$ + X=CH_2; X=CH_2, O, S and the $R^\bullet$ + O=CH_2 series) have been studied previously,[12,29,33] although not at all of the levels of theory included in the present table. The experimental data were taken from refs 31 and 32 and corrected to 0 K using temperature corrections calculated at the B3LYP/6-31G(d) level. The uncertainties in the experimental values could not be calculated exactly as they were not reported for all species in the reaction. On the basis of those that were reported, they are at least 4 kJ mol^{-1} for reactions involving CH_2=CH_2 and CH_2=O, and 14 kJ mol^{-1} for the reaction involving CH_2=S. [b] The relative value of the reaction enthalpy was calculated as the difference between it and the corresponding value for R = CH_3. In calculating the MADs of the relative values, the R = CH_3 data were omitted as their MADs are equal to zero by definition.

TABLE 3: RCH(Ph)−X Bond Dissociation Energies (0 K, kJ mol^{-1})[a] for R = CH_3, CH_2CH_3, $CH(CH_3)_2$, $C(CH_3)_3$, CH_2F, CH_2OH and CH_2CN, and X = H and F

X−CH(Ph)R	RHF	PBE	BLYP	B3LYP	B3P86	KMLYP	B1B95	MPWPW91	MPW1B95	BB1K	MPW1K	MPWB1K	BMK	RMP2	G3(MP2)-RAD	expt
H−CH(Ph)CH_3	293.7	334.6	333.3	343.7	354.4	352.5	346.7	333.4	349.0	349.6	339.7	351.3	355.5	357.8	360.4	363.1 ± 6.3
H−CH(Ph)CH_2CH_3	295.4	337.1	335.5	345.9	356.7	355.0	348.8	335.8	351.2	351.7	342.1	353.4	357.7	360.7	362.6	354.3
H−CH(Ph)$CH(CH_3)_2$	297.5	338.8	335.1	346.7	358.7	359.2	351.8	336.8	354.7	355.2	344.4	357.3	360.6	364.4	366.0	
H−CH(Ph)$C(CH_3)_3$	307.6	349.7	345.5	357.3	369.5	370.6	362.8	347.6	365.8	366.3	355.6	368.5	371.5	376.2	377.2	
H−CH(Ph)CH_2F	303.0	343.1	340.0	351.8	363.7	364.0	356.5	341.5	359.1	360.1	350.0	361.9	365.4	366.6	369.3	
H−CH(Ph)CH_2OH	303.7	345.4	341.4	353.3	365.7	365.9	358.9	343.6	361.5	362.4	351.9	364.3	367.6	370.2	371.6	
H−CH(Ph)CH_2CN	302.6	343.5	341.8	352.3	363.3	361.4	355.2	342.3	357.6	358.1	348.6	359.8	364.6	367.1	368.6	
F−CH(Ph)CH_3	297.4	429.9	408.4	404.5	420.0	441.8	418.0	422.9	422.7	409.5	389.0	413.5	425.3	457.3	424.8	
F−CH(Ph)CH_2CH_3	298.1	431.5	409.4	405.8	421.6	444.2	419.7	424.2	424.7	411.3	390.6	415.6	427.0	459.9	426.9	
F−CH(Ph)$CH(CH_3)_2$	298.5	430.8	406.5	404.3	421.4	446.9	421.1	422.7	426.7	413.4	391.1	418.2	428.3	462.1	429.1	
F−CH(Ph)$C(CH_3)_3$	307.6	441.4	416.6	414.5	431.8	457.7	432.1	433.3	437.7	424.4	401.7	429.2	438.8	473.8	440.2	
F−CH(Ph)CH_2F	301.5	432.6	409.2	406.4	423.5	445.8	421.3	425.5	425.8	413.3	393.5	417.1	429.2	460.1	427.7	
F−CH(Ph)CH_2OH	307.7	439.1	416.7	413.5	429.6	452.4	428.0	431.8	432.7	419.8	399.2	423.9	435.3	465.5	433.6	
F−CH(Ph)CH_2CN	293.3	428.7	405.6	401.7	418.2	440.1	416.1	421.2	421.1	407.5	386.8	411.8	424.0	459.5	425.0	
								Absolute Values								
mean abs dev	98.2	15.0	24.1	20.1	6.1	12.0	10.4	15.7	6.6	12.9	28.5	9.8	2.8	17.4	0	
max dev	132.6	27.5	31.6	25.7	8.4	18.8	14.3	29.6	11.4	17.5	38.5	13.2	5.6	34.5	0	
								Relative Values[b]								
mean abs dev.	2.0	1.2	2.8	2.0	1.2	1.2	0.8	1.7	0.6	0.8	1.3	0.8	0.9	0.9	0	
max dev	5.2	3.9	7.2	5.4	3.6	2.6	2.1	5.0	1.8	2.2	2.7	1.9	1.9	2.0	0	

[a] All calculations were performed using B3LYP/6-31G(d) optimized geometries and incorporate scaled B3LYP/6-31G(d) zero-point energy corrections. All single-point energy calculations except those at the G3(MP2)-RAD level were performed using the 6-311+G(3df,2p) basis set. The experimental data were taken from ref 31 and corrected to 0 K using temperature corrections calculated at the B3LYP/6-31G(d) level. [b] The relative value of the reaction enthalpy was calculated as the difference between it and the corresponding value for R = CH_3. In calculating the MADs of the relative values, the R = CH_3 data were omitted as their MADs are equal to zero by definition.

$RXCH_2^{\bullet} \rightarrow R^{\bullet} + X{=}CH_2$ and $RCH_2CH(Ph)^{\bullet} \rightarrow R^{\bullet} + CH_2{=}CH(Ph)$ (X = CH_2, O, and S; R= CH_3, CH_2CH_3, $CH(CH_3)_2$, and $C(CH_3)_3$) (Table 2). We also examine homolytic BDEs of molecules in which the R-substituents being varied are in the β rather than the α position to the breaking bond (RCH(Ph)−F and RCH(Ph)−H; R = CH_3, CH_2CH_3, $CH(CH_3)_2$, $C(CH_3)_3$, CH_2F, CH_2OH, CH_2CN, and benzyl) (Table 3). On the basis of these prototypical studies, we identify methods suitable for studying larger molecules, which we then test in a series of practical case studies. Before examining the performance of the lower cost computational methods for these radical reactions, we first examine the performance of our benchmark level of theory, G3(MP2)-RAD.

Benchmark Data. Owing to the paucity of experimental data for the thermodynamics of larger radical reactions, in the present work, we use calculations performed using the high-level ab initio method, G3(MP2)-RAD,[9] as our benchmark. This is one of the highest levels of theory that can be practically applied across all of the molecules in this paper using our current computational resources. It is a composite method, based on the G3 procedures of Curtiss et al.[27] but designed for use with radicals, that approximates (UR)CCSD(T) calculations with a large triple-ζ basis set via additivity corrections at the (RO)-MP2 level of theory.[9] It also includes spin orbit corrections for atoms and a small higher-level correction term that cancels entirely from the relative values of the reaction energies studied in this paper.

Previous assessment studies for prototypical systems indicate that this level of theory should provide a reliable benchmark for the radical reactions studied in this paper. For example, in testing against the G2/97 test set, G3(MP2)-RAD was found to have an overall mean absolute deviation (MAD) of 5.17 kJ mol^{-1}.[9] Assessment studies for prototypical radical addition and abstraction reactions have found that it generally provides an excellent approximation to experiment and to higher-level methods such as W1, with errors typically within 5 kJ mol^{-1}.[2,12,28] One exception to this is the case of radical addition to thiocarbonyl compounds, where the errors at G3(MP2)-RAD have been found to be somewhat larger than this (closer to 12 kJ mol^{-1}).[29] However, these errors were found to cancel from the relative values of the reaction enthalpies to the extent that accurate absolute values of the enthalpies could be obtained if the G3(MP2)-RAD values were corrected to the W1 level via an ONIOM approach by using W1 values for the prototypical reaction, $^{\bullet}CH_3 + S{=}CH_2 \rightarrow CH_3SCH_2^{\bullet}$.[30] Thus, even in these problematic cases, G3(MP2)-RAD should be suitable for the study of substituent effects, as in the present work.

For the present work, it is possible to compare the G3(MP2)-RAD results with experiment[31,32] for 34 of the 112 reactions studied. In those cases, G3(MP2)-RAD generally reproduces experiment with reasonable accuracy. Thus, the MAD of G3-(MP2)-RAD versus experiment is 6.4 kJ mol^{-1} for the BDEs in Table 1 and 6.2 kJ mol^{-1} for β-scission energies in Table 2, and is 6.1 kJ mol^{-1} overall. Importantly, where larger deviations do occur, they are typically less than or close to the quoted experimental uncertainties and/or occur in systems for which there is large variation among alternative experimental values. For example, the largest deviation between G3(MP2)-RAD and experiment (19.9 kJ mol^{-1}) occurs for the C−H BDE of H−C$(CH_3)_2$Ph. However, published experimental C−H BDEs for this system range from 348.1−365.3 at 298 K (338.3−355.5 at 0 K).[31] Taking an alternative experimental value as our benchmark, the error at G3(MP2)-RAD collapses to just 2.7 kJ mol^{-1}, well within the quoted uncertainty of the experimental

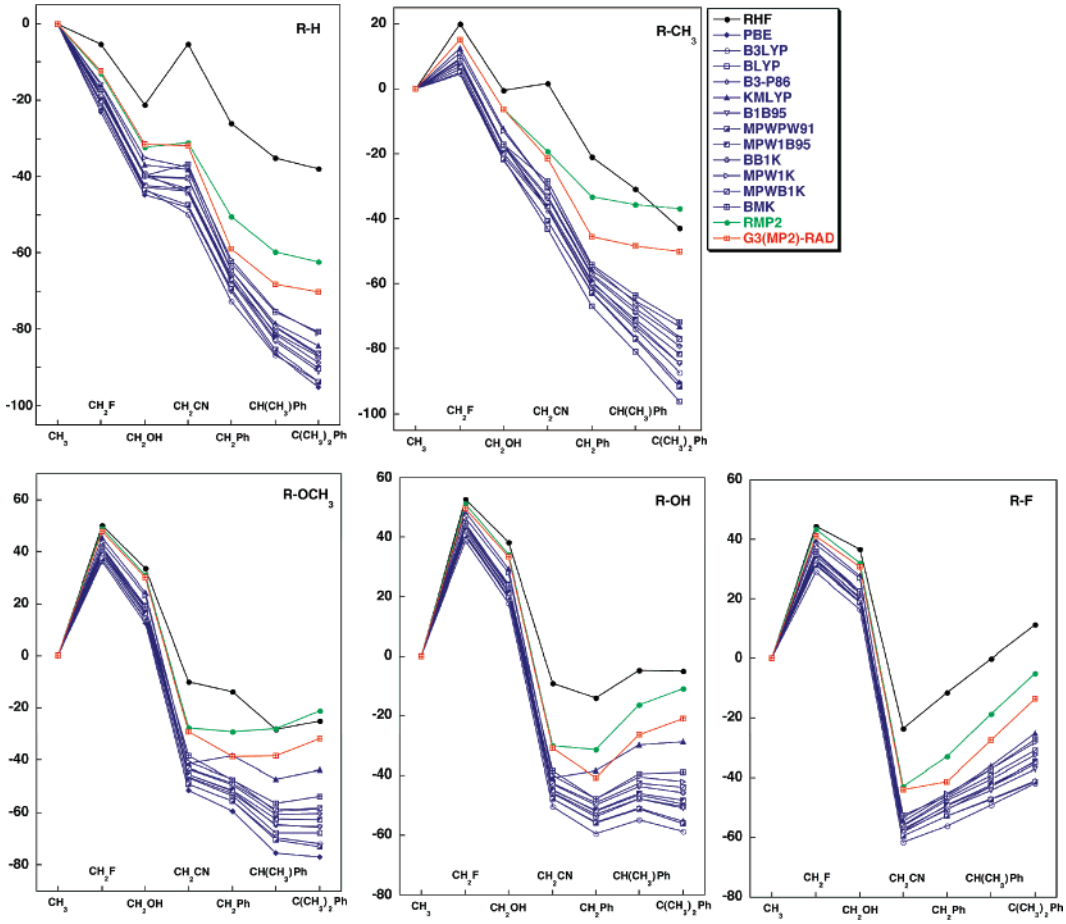

Figure 1. Effect of level of theory on the relative bond dissociation energies (kJ mol^{-1}) for the R−X species (R = CH_3, CH_2F, CH_2OH, CH_2CN, CH_2Ph, $CH(CH_3)Ph$, $C(CH_3)_2Ph$; X = H, CH_3, OCH_3, OH, F).

number. Problems with the experimental C−H BDE of H−$C(CH_3)_2$Ph, and hence the radical heat of formation of $^{\bullet}C(CH_3)_2Ph$, may also explain the second largest deviation between experiment and G3(MP2)-RAD, that for the C−F BDE of F−$C(CH_3)_2$Ph (16.4 kJ mol^{-1}). There is even wide variation among alternative experimental values of the heats of formation for some of the closed-shell species used to calculate the experimental reaction energies in the present work. For example, alternative values of the heats of formation at 298 K of CH_2═O are −115.90 and −108.6 kJ mol^{-1} and for CH_2═S are 118 and 90 kJ mol^{-1}.[32] Once errors such as these are taken into account, it is clear that, where comparison is possible, G3(MP2)-RAD does reproduce experimental values within experimental uncertainty.

It should be noted that the best-performing DFT method, BMK, also reproduces the experimental data to within a similar level of accuracy for the 34 reactions for which testing is possible. The overall MAD versus experiment for BMK (5.9 kJ mol^{-1}) is slightly lower than that for G3(MP2)-RAD (6.1 kJ mol^{-1}), although if the experimental data for the two problematic cumyl BDEs (discussed above) are omitted, the trend is reversed (in that case, the MAD of G3(MP2)-RAD versus experiment over the remaining 32 reactions is 5.4 kJ mol^{-1} compared with 5.8 kJ mol^{-1} for BMK). Although this DFT method shows similar performance versus experiment to G3(MP2)-RAD for the reactions for which testing is possible, this is not to say that the method yields similar results over the wider test set. Indeed, as will be shown below, this method deviates from G3-(MP2)-RAD by as much as 40 kJ mol^{-1} and yields significantly different chemical trends for a number of the systems studied. Rather, there are insufficient experimental data to discriminate between the methods, particularly for the larger substituted systems that were less closely related to those for which the DFT method was parametrized.

In summary, while the experimental results support the benchmark level of theory, G3(MP2)-RAD, it must be acknowledged that there are insufficient experimental data for the reactions of the present work to discriminate between this level of theory and the best-performing DFT method, BMK. In the absence of other information, we use G3(MP2)-RAD as our benchmark on the basis that it is the highest level of theory studied, does not rely upon extensive empirical parametrization, and is supported by previous assessment studies of the prototypical reactions.[2,9,12,28,29]

Prototypical Study. Initially, we compared the performance of the various levels of theory in prototypical homolysis and β-scission reactions. Figure 1 shows the relative R−X bond dissociation energies at various levels of theory for R = CH_3, CH_2F, CH_2OH, CH_2CN, benzyl, 1-phenylethyl, and cumyl, and X = H, CH_3 OCH_3, OH, and F. Figure 2 shows the relative $RXCH_2^{\bullet}$ β-scission energies for R = CH_3, CH_3CH_2, $CH(CH_3)_2$, and $C(CH_3)_3$ and X = CH_2, O, and S. The β-scission energies of $RCH_2CHPh^{\bullet} \rightarrow R^{\bullet} + CH_2$═CHPh are also included in Figure 2 so as to examine the effect of having a phenyl-substituent at the radical center. For all reactions, the relative BDEs and β-scission energies were calculated as the difference between the absolute reaction energy and the corresponding value for the same reaction but with R = CH_3; the absolute BDEs and β-scission energies are provided in Tables 1 and 2, respectively. The MADs and maximum absolute deviations from G3(MP2)-

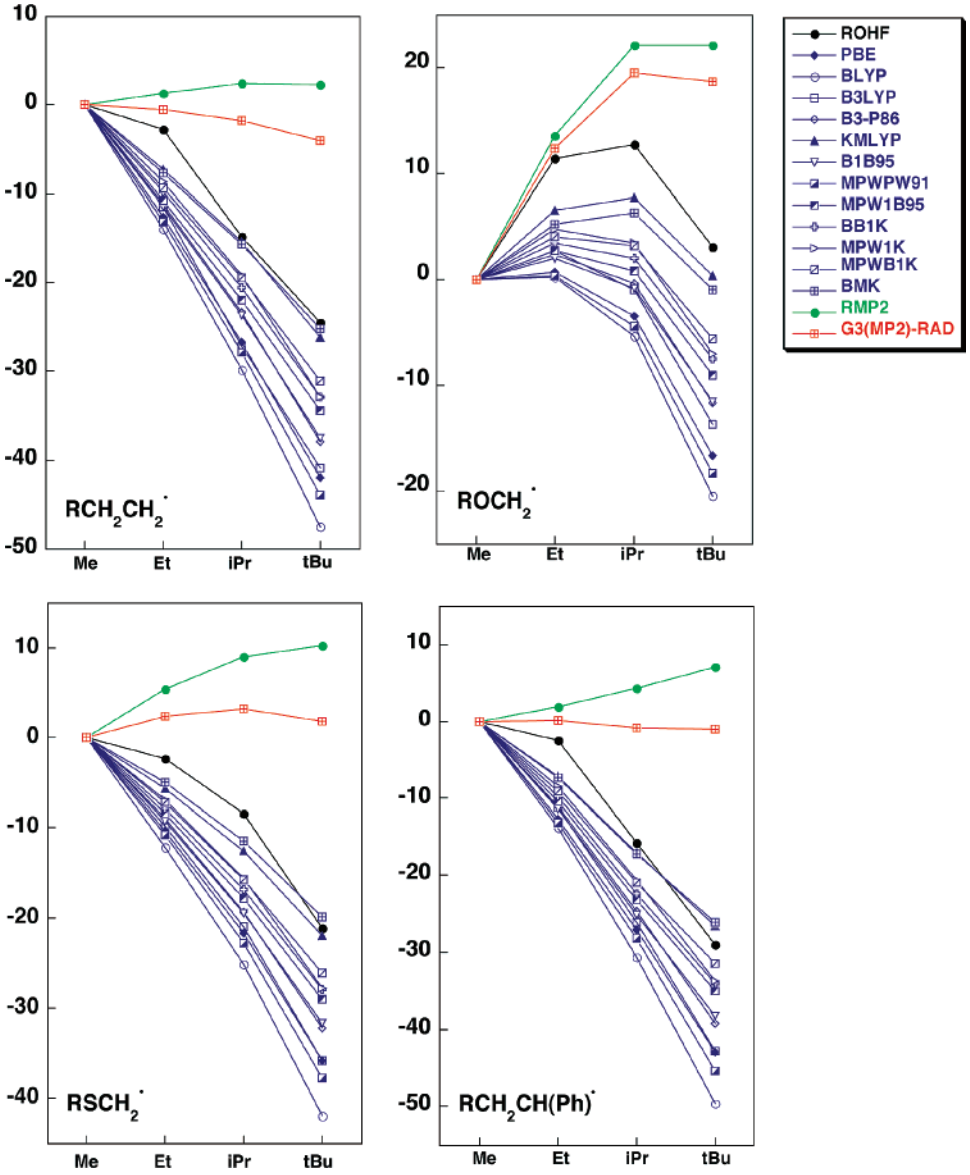

Figure 2. Effect of level of theory on the relative bond dissociation energies (kJ mol^{-1}) for the R−XCH$_2$• species (R = Me, Et, *i*-Pr, *t*-Bu; X = CH$_2$, O, S).

RAD for both the absolute values of the reaction energies, and also the relative values, are also provided in these tables. The geometries of all species are provided in the Supporting Information. It should be noted that the R = CH$_3$ reactions for a number of these systems have been studied previously[2,12,29,33] but are included here as the reference values. In addition, a preliminary study of the ROCH$_2$• β-scission reactions was reported in ref 33 but has been expanded for the present work to include a wider range of DFT methods.

From Tables 1 and 2, it is seen that all low-cost methods fail to provide accurate values when compared with the G3(MP2)-RAD benchmark values. Of the DFT methods, BMK shows the best performance, having mean absolute deviations (MAD) from G3(MP2)-RAD of 6.3 kJ mol^{-1} for the BDEs and 8.3 kJ mol^{-1} for the β-scission energies. However, even this method is subject to large and variable deviations from G3(MP2)-RAD; for example, its signed deviations from G3(MP2)-RAD range from −25.7 to 10.1 kJ mol^{-1} for the BDEs in Table 1, and from −13.9 to 21.8 kJ mol^{-1} for the β-scission energies of Table 2.

These nonsystematic deviations from G3(MP2)-RAD become clearly apparent when the relative values of the BDEs (Figure 1) and β-scission energies (Figure 2) are examined. All of the DFT methods tested fail to model correctly the effects of substituents on these reactions to the extent that, in the case of the β-scission energies, the methods even yield the incorrect qualitative trends in the data when compared with G3(MP2)-RAD. This is also reflected in the mean and maximum absolute deviations for the relative values of the enthalpies, which, for the DFT methods, are either similar to or in many cases more than those for the corresponding absolute values. This is in contrast to the ab initio methods studied, RHF and RMP2, where there is substantial systematic cancellation of errors from the relative values of reaction energies as more of the chemistry (i.e., functional groups, chemical bonds, etc.) is conserved and may be related to the empirical parametrization of the DFT methods. It is therefore clear that the deviations between high-level ab initio methods and contemporary DFT methods are not systematic and not limited to the BDEs of simple closed-shell compounds.

What is significant and disappointing about the present results is the performance of the ab initio method RMP2/6-311+G-(3df,2p). In contrast to our previous study of the simple alkyl radicals, this method also fails to model the substituent effects

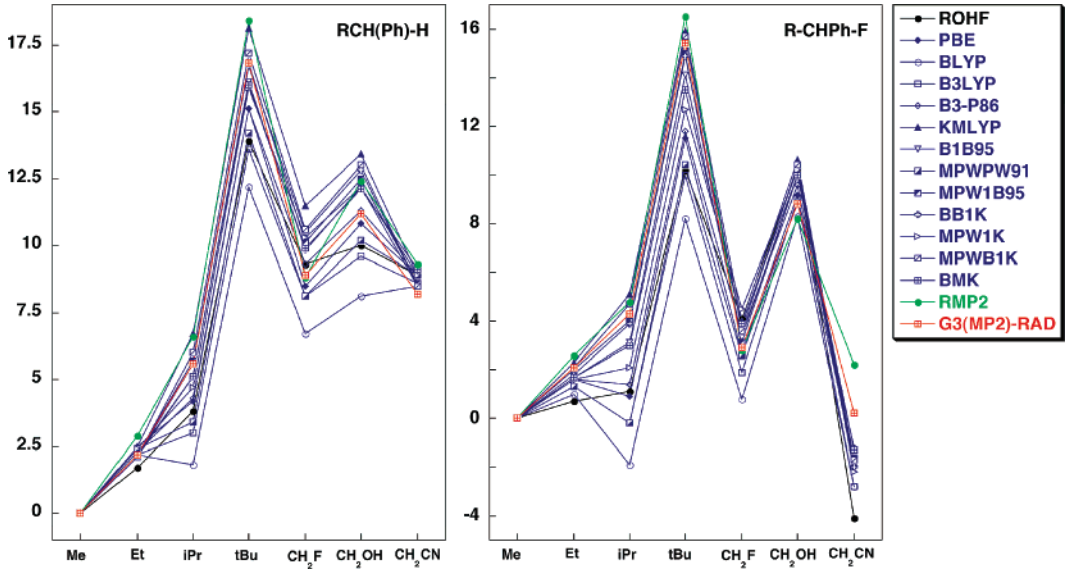

Figure 3. Effect of level of theory on the relative bond dissociation energies (kJ mol^{-1}) for the RCHPh−X species (R = CH_3, CH_3CH_2, $CH(CH_3)_2$, $C(CH_3)_3$, CH_2F, CH_2OH, CH_2CN; X = H, CH_3, OCH_3, OH, F).

on the BDEs in some cases, particularly when R bears substituents such as phenyl that interact strongly with the unpaired electron. The method also overestimates the bond-weakening effects of increasing alkylation in the β-scission reactions both with and without the phenyl substituent at the radical center. We have previously observed the failure of RMP2 methods in other reactions involving delocalized radicals such as benzyl and cyanoisopropyl.[3,34] For example, in our studies of radical addition to C=S bonds, we found that RMP2/6-311+G(3df,2p) correctly modeled the effect of R (relative to R = CH_3) on the enthalpies of the reaction $R^\bullet$ + S=$C(CH_3)$-SCH_3 → $RSC^\bullet(CH_3)SCH_3$ for R = CH_2CH_3, CH_2COOCH_3, $CH(CH_3)COOCH_3$, and CH_2OCOCH_3 (MAD = 3.1 kJ mol^{-1}) but the errors for R-groups containing phenyl or cyano α-substituents (R = CH_2Ph, $CH(CH_3)Ph$, $C(CH_3)_2Ph$, CH_2CN, and $C(CH_3)_2CN$) were nearly three times higher (MAD = 9.6 kJ mol^{-1}).[35] Although these errors were found to be considerably smaller than those for the best of the DFT methods tested (in that case BMK, whose MAD was 23.8 kJ mol^{-1} for the same systems),[3,35] they were nonetheless unacceptably high for quantitative studies. The observed errors in the MP2 calculations of delocalized radicals are no doubt related to the well-known slow convergence of Møller−Plesset perturbation theory in systems having small HOMO−LUMO gaps.[36]

ONIOM. In the light of this failure of both RMP2 and the DFT methods to reproduce the substituent effects on BDEs and β-scission energies when compared with our benchmark values, it becomes pertinent to seek alternative low-cost methods for studying larger systems. In the long term, we hope that with further improvements, DFT methods may yet fulfill this role. In this regard, we note that the recently introduced M05-2X DFT method of Truhlar and co-workers has shown great promise in a number of problematic systems.[5d,37] Unfortunately, as this method is not yet widely available, we were unable to include it in the present study. Instead, we examined an alternative approach using a QM/QM version of the ONIOM method of Morokuma and co-workers.[26] In the past, we have shown that high-level methods such as G3(MP2)-RAD can be well approximated by calculations in which only the core of the reaction is treated by using a high-level composite procedure and a lower cost method is used merely to model the remaining substituent effects on the chemical reaction.[3] However, the success of this approach depends upon the ability of the low-cost method to model remote substituent effects. As we have seen above, neither DFT methods nor RMP2 methods are capable of modeling the effect of substituents α to the reaction center when compared with the benchmark values.

To investigate whether any of the low-cost methods tested could model more remote substituent effects, we examined the performance of the various levels of theory for modeling the effects of R on the RCH(Ph)−X BDEs for R = CH_3, CH_2CH_3, $CH(CH_3)_2$, $C(CH_3)_3$, CH_2F, CH_2OH, and CH_2CN and X = H and F. In these systems, the reaction center contains an α phenyl group that, as seen above, is difficult to model accurately using RMP2, but within a series, this α substituent is held constant and only the remote substituents are varied. The absolute BDEs are provided in Table 3; the corresponding relative BDEs (calculated again using R = CH_3 as the reference value) are plotted in Figure 3; the geometries of all species are provided in the Supporting Information.

If we examine first the absolute RCH(Ph)−X BDEs, we first note that, not unexpectedly, the RMP2 method shows large deviations from G3(MP2)-RAD (MAD = 17.4 kJ mol^{-1}), reflecting its problems in modeling radicals with α-phenyl substituents. All of the DFT methods tested also show deviations from G3(MP2)-RAD, although in the case of the best-performing DFT method, BMK, these errors are relatively small (MAD = 2.8 kJ mol^{-1}, max deviation = 5.7 kJ mol^{-1}). While it would be tempting to adopt BMK on the basis of these results, it must be remembered that this same method showed large and seemingly unpredictable deviations from G3(MP2)-RAD (as much as 25.7 kJ mol^{-1}) in some of the other BDEs examined above. Until the specific causes of these deviations are identified, it is difficult to predict its level of error for new, untested radical reactions.

Turning instead to the relative values of the BDEs (Figure 3), we note that all of the low-cost methods show greatly improved performance in modeling the substituent effects on the RCH(Ph)−X BDEs now that the substituents that are being varied (R) are remote to the reaction center. This improved performance can be exploited in building an ONIOM-based method for calculating the reaction energies. As noted above, the ONIOM method was introduced by Morokuma and co-workers[26] as a QM/MM approach to studying larger biological systems. However, applying the same basic principles, it is possible to calculate QM/QM single-point energies of a molecule

TABLE 4: Performance of ONIOM for the RCH(Ph)−X Bond Dissociation Energies (0 K, kJ mol^{-1})[a] for R = CH_3, CH_2CH_3, $CH(CH_3)_2$, $C(CH_3)_3$, CH_2F, CH_2OH, and CH_2CN and X = H and F[a]

	ONIOM calculation												
X−CH(Ph)R	RHF	PBE	BLYP	B3LYP	B3P86	KMLYP	B1B95	MPWPW91	MPW1B95	BB1K	MPW1K	MPWB1K	BMK	RMP2	G3(MP2)-RAD
H−CH(Ph)CH_3	360.4	360.4	360.4	360.4	360.4	360.4	360.4	360.4	360.4	360.4	360.4	360.4	360.4	360.4	360.4
H−CH(Ph)CH_2CH_3	362.1	362.9	362.6	362.6	362.7	362.9	362.5	362.8	362.6	362.5	362.8	362.5	362.6	363.3	362.6
H−CH(Ph)$CH(CH_3)_2$	364.2	364.6	362.2	363.4	364.7	367.1	365.5	363.8	366.1	366.0	365.1	366.4	365.5	367.0	366.0
H−CH(Ph)$C(CH_3)_3$	374.3	375.5	372.6	374.0	375.5	378.5	376.5	374.6	377.2	377.1	376.3	377.6	376.4	378.8	377.2
H−CH(Ph)CH_2F	369.7	368.9	367.1	368.5	369.7	371.9	370.2	368.5	370.5	370.9	370.7	371.0	370.3	369.2	369.3
H−CH(Ph)CH_2OH	370.4	371.2	368.5	370.0	371.7	373.8	372.6	370.6	372.9	373.2	372.6	373.4	372.5	372.8	371.6
H−CH(Ph)CH_2CN	369.3	369.3	368.9	369.0	369.3	369.3	368.9	369.3	369.0	368.9	369.3	368.9	369.5	369.7	368.6
F−CH(Ph)CH_3	424.8	424.8	424.8	424.8	424.8	424.8	424.8	424.8	424.8	424.8	424.8	424.8	424.8	424.8	424.8
F−CH(Ph)CH_2CH_3	425.5	426.4	425.8	426.1	426.4	427.1	426.5	426.1	426.8	426.6	426.4	426.9	426.5	427.4	426.9
F−CH(Ph)$CH(CH_3)_2$	425.9	425.7	422.9	424.6	426.2	429.9	427.9	424.6	428.8	428.7	426.9	429.5	427.8	429.6	429.1
F−CH(Ph)$C(CH_3)_3$	435.0	436.3	433.0	434.8	436.6	440.7	438.9	435.2	439.8	439.7	437.5	440.5	438.3	441.3	440.2
F−CH(Ph)CH_2F	428.9	427.5	425.6	426.7	428.3	428.8	428.1	427.4	427.9	428.6	429.3	428.4	428.7	427.6	427.7
F−CH(Ph)CH_2OH	435.1	434.0	433.1	433.8	434.4	435.4	434.8	433.7	434.8	435.1	435.0	435.2	434.8	433.0	433.6
F−CH(Ph)CH_2CN	420.7	423.6	422.0	422.0	423.0	423.0	422.9	423.1	423.2	422.8	422.6	423.1	423.5	427.0	425.0
mean abs dev	2.0	1.2	2.8	2.0	1.2	1.2	0.8	1.7	0.6	0.8	1.3	0.8	0.9	0.9	0.0
max dev	5.2	3.9	7.2	5.4	3.6	2.6	2.1	5.0	1.8	2.2	2.7	1.9	1.9	2.0	0.0

[a] All calculations were performed using B3LYP/6-31G(d) optimized geometries and incorporate scaled B3LYP/6-31G(d) zero-point energy corrections. All single point energy calculations except those at the G3(MP2)-RAD level were performed using the 6-311+G(3df,2p) basis set. The ONIOM values were calculated using G3(MP2)-RAD for the core reaction (defined as the BDE for R = Me) and the various low-cost levels of theory for the substituent effect. The pure G3(MP2)-RAD values are included for purposes of comparison. In calculating the MADs, the R = CH_3 data were omitted as their MADs are equal to zero by definition.

as a linear combination of the single- point energy of the core and the substituent of the rest of the system. For each series of reactions (i.e., RCH(Ph)−H and RCH(Ph)−F), values of the BDEs were calculated by using an ONIOM method in which the core reaction was defined as the BDE for the R = CH_3 case and was studied at G3(MP2)-RAD, and the substituent effect of the R-group was then studied at a lower level. In essence, the core reaction includes all substituents that are α to the reaction center but neglects all substituents at the β position and beyond. Because in the present work, the geometries of the core reaction and full system are fully optimized at the same level of theory, the ONIOM values are effectively a linear combination of the BDE for the reference reaction (measured at G3(MP2)-RAD) and the relative BDE of the full system (measured at a low level of theory). Table 4 shows the resulting ONIOM values obtained when the different low levels of theory were used to study the substituent effect.

From Table 4, it would appear that all of the low-cost methods (including RHF) provide sufficiently accurate measures of the remote substituent effects in these reactions for constructing ONIOM energies to within an MAD of 2.8 kJ mol^{-1} (or less) of G3(MP2)-RAD. In practice, the RHF and some of the older functionals such as BLYP, B3LYP, and MPWPW91 would probably not be considered sufficiently reliable for general use as the maximum deviations in their ONIOM values still exceed 4 kJ mol^{-1}. Nonetheless, for RMP2 and most of the DFT procedures, the maximum errors in their ONIOM values are approximately 2 kJ mol^{-1} and the MADs are even smaller. This excellent performance is encouraging, particularly given that the substituent effects being measured are not negligible and that many of these methods showed very large deviations when used to calculate the absolute values of the BDEs.

It therefore appears that, although none of the low levels of theory tested provide *consistently* accurate values of the enthalpies of radical reactions when compared with G3(MP2)-RAD, these values can be well approximated by using an ONIOM method in which only the core reaction is studied at G3(MP2)-RAD and the full system is studied at a lower level of theory such as RMP2 or a modern DFT procedure such as BMK. This greatly reduces the computational cost of the calculation without compromising its accuracy. The success of the approach depends upon the choice of the core reaction. The present work indicates that it is sufficient that only substituents α to the reaction center are included; however, in the systems studied, the remote substituents are not conjugated with the reaction center and functional groups such as phenyl are treated as single intact units. In systems where the remote substituents are capable of interacting strongly with the reaction center, it is possible that the core reaction and/or the level of theory chosen for the measuring substituent effect may need to be adjusted. For example, in our studies of RAFT reactions, we have found that while RMP2 is capable of modeling the effect of the remote substituent R′ on the enthalpy of the addition reaction $^{\bullet}CH_3 + S{=}C(CH_3)SR' \rightarrow CH_3SC^{\bullet}(CH_3)SR'$, the DFT procedures tested (including BMK) show errors of as much as 10 kJ mol^{-1} (see Figure 4; the raw data for this Figure are taken from ref 3). It is therefore advisable to test the accuracy of the ONIOM approach in cases where the remote substituents are capable of interacting strongly with the reaction and, if necessary, revise the core system and low-cost level of theory accordingly. In that regard, RMP2 appears thus far to be the most reliable of the low-cost procedures, although it of course is also more computationally expensive than its DFT counterparts.

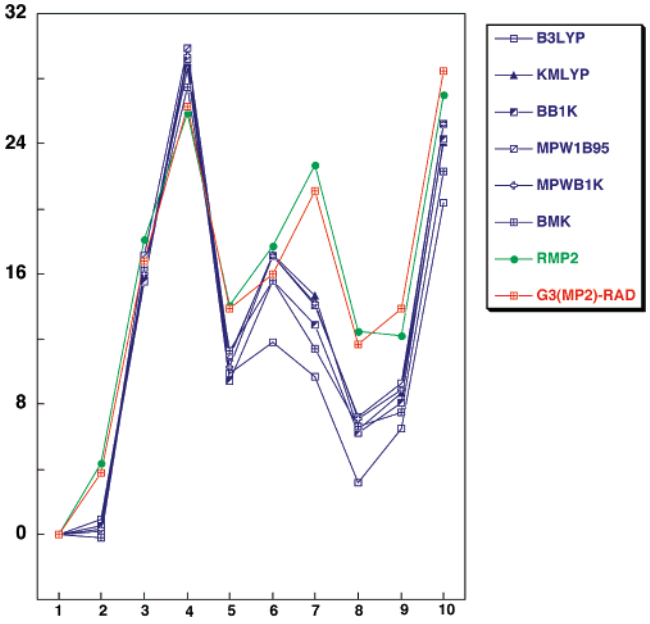

Figure 4. Performance of various levels of theory for measuring the effect of R′ on enthalpy of R′SC•$(CH_3)SCH_3$ → R′SC(CH_3)═S + •-CH_3 (relative to R′ = CH_3). Data from ref.[3] (The R′ substituents are labeled as follows: 1, CH_3; 2, CH_2CH_3; 3, CH_2Ph; 4, CH_2COOCH_3; 5, CH_2CN; 6, CH_2OCOCH_3; 7, $CH(CH_3)PH$; 8, $CH(CH_3)COOCH_3$; 9, $C(CH_3)_2CN$; 10, $C(CH_3)_2CN$).

Practical Case Studies. On the basis of the above studies of prototypical systems, it appears that an ONIOM method in which the core reaction is treated at G3(MP2)-RAD and the (remote) substituent effect is treated with a low-cost method such as RMP2/6-311+G(3df,2p) or BMK/6-311+G(3df,2p) offers a computationally efficient route to accurate radical thermochemistry. To test the accuracy of this ONIOM approach in larger and more practical applications and to identify which low-cost method is most suitable for modeling the substituent effect, we have examined a series of case studies. The systems studied included the alkyl-oxygen BDEs of nitroxides (R−TEMPO → R• + TEMPO•; R = CH_3, CH_2CH_3, $CH(CH_3)_2$, $C(CH_3)_3$, $CH_2CH_2CH_3$, CH_2F, CH_2OH, CH_2CN, $CH(CN)CH_3$, $CH(Cl)CH_3$; TEMPO = 2,2,6,6,-tetramethylpiperidin-1-yloxyl; see Table 5), the alkyl-halogen BDEs of a series of oligomeric halides relevant to the initiation of atom transfer radical polymerization (HM_1M_2−X; M_1, M_2 = $CH_2CH(CH_3)$ (P), CH_2-$CH(COOCH_3)$ (MA), and $CH_2C(CH_3)(COOCH_3)$ (MMA) and X = Cl and Br; see Table 6), and a series of additional radical reactions including addition, ring-opening, and hydrogen and halogen transfer (see Table 7; the reactions are shown Scheme 1). For all reactions, calculations were performed at all of the low-cost RHF, RMP2, and DFT methods examined above, and ONIOM procedures in which the core was treated at G3(MP2)-RAD and the substituent effect was treated at B3LYP/6-311+G-(3df,2p), BMK/6-311+G(3df,2p), or RMP2/6-311+G(3df,2p). Unless noted otherwise, the core reaction contained all substituents α to the reaction center but omitted all remote substituents. In all cases, hydrogens were used as link atoms and the geometries of the core and full system were both fully optimized at the same level of theory used throughout this work, B3LYP/6-31G(d). The corresponding G3(MP2)-RAD benchmark calculations for all reactions are also provided; those for Table 6[38] and reactions 6−8 of Table 7[39] were taken from earlier studies. The geometries of all species are included in the Supporting Information, with the exception of those in Table 6, which are provided in an earlier publication.[38]

TABLE 5: R−TEMPO → R• + •TEMPO Bond Dissociation Energies (0 K, kJ mol^{-1})[a]

														ONIOM-B3LYP		ONIOM−BMK		ONIOM-RMP2		G3(MP2)-RAD
R•	RHF	PBE	BLYP	B3LYP	B3P86	KMLYP	B1B95	MPWPW91	MPW1B95	BB1K	MPW1K	MPWB1K	BMK	RMP2	α	β	α	β	α	β	
•CH_3	108.0	165.0	140.6	151.0	167.9	126.5	173.7	155.7	181.4	176.7	159.1	182.9	185.8	203.9	184.3	188.0	192.3	194.4	187.0	193.2	197.8
•CH_2CH_3	118.0	164.3	138.9	151.9	168.9	130.6	174.4	154.5	183.1	179.2	162.7	186.1	190.1	219.8	195.1	199.7	203.3	206.2	201.3	207.5	211.8
•$CH(CH_3)_2$	96.9	144.6	116.2	130.8	149.5	112.9	155.1	133.3	165.1	160.7	143.2	168.7	174.7	216.5	185.1	192.1	194.5	198.8	196.6	202.8	207.1
•$C(CH_3)_3$	64.8	115.8	85.1	101.0	121.1	88.0	125.8	102.9	137.3	132.0	113.7	141.2	149.9	201.5	167.3	177.4	176.4	181.9	180.3	186.4	192.0
•$CH_2CH_2CH_3$	119.0	164.9	139.1	152.6	169.8	133.2	175.3	155.0	184.0	180.2	163.9	187.2	191.3	222.6	195.8	201.6	204.5	208.2	204.1	210.1	214.4
•CH_2F	155.3	202.0	176.6	189.8	206.7	170.5	209.8	192.3	218.6	214.8	200.6	221.9	225.7	250.4	231.0	235.0	237.6	239.8	232.2	239.1	244.4
•CH_2OH	129.9	174.9	146.9	161.1	180.4	144.4	183.2	164.9	192.3	188.9	175.2	196.1	198.4	229.6	208.1	213.9	215.6	218.8	211.8	218.1	223.3
•CH_2CN	99.7	115.7	89.7	104.8	122.3	87.6	127.4	106.6	135.8	133.2	118.6	139.8	146.5	177.4	154.5	158.8	162.5	165.0	159.3	165.7	170.3
•$CH(CN)CH_3$	88.8	105.4	76.6	93.3	111.9	80.7	116.8	94.7	126.8	123.6	108.5	131.5	140.9	182.6	153.4	160.1	163.0	167.1	163.5	169.9	174.3
•$CH(Cl)CH_3$	110.9	160.3	134.0	145.6	163.1	130.1	165.6	149.8	174.9	169.6	154.4	177.2	189.9	225.3	195.0	201.2	204.2	208.0	205.4	211.7	216.0
mean abs dev	96.0	53.9	80.8	67.0	49.0	84.7	44.5	64.2	35.2	39.3	55.2	31.9	25.8	7.8	18.2	12.4	9.7	6.3	11.0	4.7	0.0
max dev	127.2	76.2	106.9	91.1	71.0	104.0	66.2	89.1	54.7	60.0	78.3	50.8	42.2	9.5	24.7	14.9	15.6	10.2	12.2	5.6	0.0

[a] All calculations were performed using B3LYP/6-31G(d) optimized geometries and incorporate scaled B3LYP/6-31G(d) zero-point energy corrections. All single-point energy calculations except those at the G3(MP2)-RAD level were performed using the 6-311+G(3df,2p) basis set. TEMPO stands for 2,2,6,6-tetramethylpiperidin-1-yloxy. The α-ONIOM systems use H_2NO• in place of TEMPO, the β-ONIOM systems use $(CH_3)_2NO$• in place of TEMPO.

TABLE 6: $HM_1M_2-X \rightarrow HM_1M_2^{\bullet} + {}^{\bullet}X$ Bond Dissociation Energies (0 K, kJ mol^{-1}) for M_1, M_2 = $CH_2CH(CH_3)$ (P), $CH_2CH(COOCH_3)$ (MA), and $CH_2C(CH_3)(COOCH_3)$ (MMA) and X = Cl and Br[a]

															ONIOM			
HM_1M_2-X	RHF	PBE	BLYP	B3LYP	B3P86	KMLYP	B1B95	MPWPW91	MPW1B95	BB1K	MPW1K	MPWB1K	BMK	RMP2	B3LYP	BMK	MP2	G3(MP2)-RAD
HP−Cl	254.9	348.9	317.7	321.1	342.9	371.6	345.6	340.3	350.4	343.6	328.2	347.6	357.6	367.8	348.3	348.3	348.3	348.3
HPP−Cl	251.4	348.5	316.0	319.8	342.3	372.4	345.7	339.3	351.0	344.0	327.6	348.3	358.4	370.4	346.1	348.1	349.9	349.9
HMAP−Cl	258.2	350.7	317.8	322.5	345.4	377.0	349.7	341.6	355.1	348.5	331.3	352.9	361.8	373.3	348.7	351.5	352.8	353.3
HMMAP−Cl	241.4	339.2	305.6	309.7	332.5	363.8	337.0	329.4	342.8	335.4	317.8	340.2	349.9	364.5	336.9	340.5	345.0	344.7
HMA−Cl	217.5	303.5	271.5	275.8	297.6	325.5	300.0	295.2	304.7	298.4	284.8	302.3	313.4	328.4	308.9	308.9	308.9	308.9
HPMA−Cl	214.5	302.5	269.1	274.1	296.7	326.3	299.9	293.7	305.1	298.6	284.0	302.9	313.4	331.0	306.7	308.3	311.0	310.5
HMAMA−Cl	218.2	307.2	273.0	278.3	301.6	331.6	304.7	298.3	309.9	303.4	288.7	307.8	317.7	334.2	310.0	311.8	313.3	314.1
HMMAMA−Cl	204.6	298.0	261.3	267.4	290.7	324.5	296.0	287.0	302.9	295.1	277.8	300.8	310.3	334.3	300.5	305.7	314.7	310.0
HMMA−Cl	211.9	291.1	258.2	263.9	286.4	317.1	288.9	282.5	294.3	288.4	275.1	292.8	305.8	327.4	306.5	306.5	306.5	306.5
HPMMA−Cl	200.2	284.1	248.0	255.0	279.3	313.5	283.8	274.2	290.2	283.9	268.0	289.2	300.2	324.1	297.6	300.8	303.2	302.2
HMAMMA−Cl	196.1	283.7	245.6	252.8	277.1	313.1	283.4	272.3	290.9	283.4	265.7	289.6	300.3	330.7	295.1	300.7	309.5	307.1
HMMAMMA−Cl	195.3	280.6	245.2	251.5	276.0	307.6	279.7	271.6	285.3	279.3	264.4	283.9	295.1	320.1	293.1	294.8	298.2	299.0
HP−Br	419.2	297.5	268.3	270.4	290.7	317.8	291.4	289.6	296.2	289.0	276.6	293.1	292.3	327.0	294.9	294.9	294.9	294.9
HPP−Br	415.3	296.6	264.9	267.9	289.6	318.8	291.8	287.7	297.2	289.8	275.5	294.3	292.6	331.7	291.4	294.3	298.7	298.0
HMAP−Br	421.7	299.1	267.5	271.1	292.9	323.2	295.3	290.4	300.8	293.7	279.3	298.3	295.6	333.3	294.5	297.2	300.2	300.5
HMMAP−Br	405.2	287.7	255.9	258.9	280.1	309.7	282.6	278.4	288.4	280.6	265.9	285.4	284.1	325.3	283.2	286.6	293.1	292.4
HMA−Br	384.4	254.6	224.4	227.7	248.1	274.8	248.6	246.9	253.5	246.7	235.9	250.7	251.1	291.7	259.1	259.1	259.1	259.1
HPMA−Br	381.5	253.7	222.1	226.1	247.3	275.6	248.7	245.4	254.0	247.2	235.2	251.5	251.1	295.7	256.8	258.4	262.5	261.5
HMAMA−Br	384.0	257.9	224.7	229.2	251.6	280.9	253.0	249.3	258.5	251.6	239.3	256.1	254.4	298.5	259.0	260.8	264.4	264.8
HMMAMA−Br	372.1	250.4	216.1	220.9	242.7	274.6	245.4	240.4	252.1	244.2	230.4	249.7	248.2	299.6	251.6	255.4	266.3	263.5
HMMA−Br	375.1	240.0	208.7	213.1	234.3	263.3	234.9	231.9	240.4	234.0	223.4	238.5	239.8	289.2	254.7	254.7	254.7	254.7
HPMMA−Br	364.0	233.2	199.4	204.4	226.9	258.4	229.4	223.8	235.8	228.8	215.4	234.0	233.7	287.8	245.4	247.9	252.7	251.5
HMAMMA−Br	361.2	232.1	196.3	202.5	225.5	259.8	229.9	221.8	237.1	229.7	214.7	235.6	233.9	291.2	243.7	248.4	256.5	254.7
HMMAMMA−Br	354.8	229.3	195.4	200.4	223.7	253.4	225.6	220.8	231.2	224.8	212.4	229.4	228.4	274.2	241.0	242.3	238.7	239.1
mean abs dev	108.1	9.4	42.4	37.7	15.3	15.2	12.4	18.2	7.3	13.6	28.0	8.9	7.7	27.6	5.0	2.9	0.8	0.0
max dev	125.4	23.4	61.5	54.2	30.0	23.7	24.9	34.7	17.6	25.0	41.4	19.1	20.9	36.5	11.9	8.1	4.8	0.0

[a] All calculations were performed using B3LYP/6-31G(d) optimized geometries and incorporate scaled B3LYP/6-31G(d) zero-point energy corrections. All RHF and RMP2 single-point energy calculations performed using the cc-pVTZ basis set, all DFT calculations performed using the 6-311+G(3df,2p) basis set. The G3(MP2)-RAD values were reported in ref 38. Experimental values (corrected to 0 K using calculated B3LYP/6-31G(d) temperature corrections) for HP−Cl and HP−Br are 350.6 ± 6.3 and 296.2 ± 6.3 kJ mol^{-1}, respectively.[31]

TABLE 7: Enthalpies of Various Addition, Ring-Opening, and Abstraction Reactions[a]

													ONIOM			
reaction	RHF	PBE	BLYP	B3LYP	B3P86	KMLYP	B1B95	MPWPW91	MPW1B95	BB1K	MPW1K	MPWB1K	BMK	RMP2	B3LYP	BMK	RMP2	G3(MP2)-RAD
1	−66.6	−87.9	−52.3	−68.8	−91.8	−120.6	−83.1	−80.2	−89.7	−91.7	−103.8	−96.9	−93.0	−101.6	−86.4	−86.8	−88.6	−88.1
2	−60.3	−72.9	−34.5	−54.7	−79.2	−114.9	−71.8	−64.0	−79.9	−82.8	−94.0	−89.0	−87.0	−104.8	−84.7	−86.9	−86.9	−90.1
3	−75.9	−89.0	−53.1	−72.2	−95.4	−130.3	−87.1	−80.5	−95.2	−97.5	−108.3	−103.8	−103.5	−120.4	−101.0	−102.2	−102.2	−105.1
4	−69.9	−69.4	−59.9	−67.5	−71.3	−91.6	−60.5	−64.3	−66.6	−64.9	−74.1	−69.7	−66.3	−90.6	−87.4	−87.8	−90.3	−89.5
5	−25.5	−9.8	−2.6	−6.1	−11.8	−12.7	−10.7	−9.0	−10.7	−12.3	−13.9	−12.1	−19.1	−31.9	−26.0	−26.2	−24.8	−24.5
6	9.0	27.6	37.1	35.3	29.5	30.5	28.6	29.2	28.3	28.2	28.4	28.1	24.8	10.6	16.1	16.5	17.2	16.9
7	−49.4	−65.1	−59.6	−61.6	−66.6	−66.7	−62.9	−64.3	−62.6	−63.3	−65.8	−63.0	−66.0	−78.0	−76.4	−71.8	−69.1	−69.0
8	−14.9	−27.8	−20.0	−20.2	−25.3	−23.5	−23.6	−26.1	−23.6	−22.8	−23.6	−22.8	−22.2	−35.4	−34.3	−29.0	−27.0	−27.5
9	3.8	−6.6	−6.8	−2.5	−1.3	6.9	−5.0	−5.8	−4.6	−1.8	4.2	−1.5	−11.0	−15.5	−10.7	−10.4	−9.8	−9.7
10	−12.3	−63.2	−64.1	−56.3	−54.4	−43.3	−54.9	−61.7	−54.2	−49.3	−44.2	−48.9	−54.6	−60.1	−59.2	−54.4	−53.1	−53.3
11	−20.2	−62.0	−63.8	−58.0	−56.1	−47.1	−57.2	−61.2	−56.5	−52.8	−47.8	−52.3	−57.9	−61.6	−61.0	−55.9	−54.1	−54.2
12	−6.7	−2.0	−3.8	−4.1	−3.0	−1.6	−3.6	−3.0	−2.5	−3.7	−4.4	−2.8	1.1	3.7	1.3	3.9	4.3	7.3
13	−14.4	−12.9	−5.9	−10.2	−15.0	−18.5	−16.9	−12.5	−16.7	−18.8	−19.2	−18.6	−10.3	−22.6	−12.1	−10.1	−14.8	−10.6
mean abs dev	19.1	8.9	20.9	14.4	7.6	12.8	10.2	11.5	8.0	8.4	9.0	7.5	5.2	8.5	3.9	1.8	1.2	0.0
max dev	41.0	20.2	55.6	35.4	18.2	32.5	29.0	26.1	22.9	24.6	15.7	19.8	23.3	15.3	7.4	3.4	4.2	0.0

[a] All calculations were performed using B3LYP/6-31G(d) optimized geometries and incorporate scaled B3LYP/6-31G(d) zero-point energy corrections. All single-point energy calculations except those at the G3(MP2)-RAD level were performed using the 6-311+G(3df,2p) basis set. Reaction numbers refer to those in Scheme 1. G3(MP2)-RAD values for reactions 5−8 were reported in ref 39. Experimental values (corrected to 0 K) for reactions 1, 5, 6, 7, and 8 are −93.2, −32.5, 12.9, −61.5, and −16.1 kJ mol^{-1}, respectively.[31,32] The uncertainties in the experimental values could not be calculated exactly as they were not reported for all species in the reaction. On the basis of those that were reported, they are at least 4 kJ mol^{-1} for reactions 1, 5, and 6, and at least 10 kJ mol^{-1} for 7 and 8.

Examining first the alkyl-oxygen BDEs of the nitroxides (Table 5), we note that all low-cost procedures show significant deviations from G3(MP2)-RAD. The deviations are particularly large for the DFT procedures with even the best-performed DFT method, BMK, having deviations of as much as 42.2 kJ mol^{-1}. Although RMP2 fares better, its deviations are still too high for quantitative applications (MAD = 7.8 kJ mol^{-1}; maximum deviation = 9.5 kJ mol^{-1}). Turning to the ONIOM values, we first note that in defining a core reaction for these systems, a decision had to be made concerning the status of the six-membered piperidinyl ring of the TEMPO species. Ideally one would treat all rings as complete functional groups and include them intact as α substituents. However, because this increases the cost of the calculation, we investigated the performance of simpler ONIOM methods in which only portions of the ring were included. Initially we examined ONIOM values that treat the TEMPO unit as $H_2NO^{\bullet}$, thereby truncating the ring at the α-position to the reaction center. However, because these values (denoted as α-ONIOM values in Table 5) were not found to be sufficiently accurate, we then examined *β*-ONIOM values that treated the TEMPO unit as $(CH_3)_2NO^{\bullet}$. In this latter case, the ONIOM method offered an excellent approximation to the G3-(MP2)-RAD values (MAD = 4.7 kJ mol^{-1}, maximum deviation = 5.6 kJ mol^{-1}), provided that the RMP2 method was used to model the substituent effect. In contrast, the ONIOM methods incorporating DFT calculations were still not sufficiently accurate for quantitative purposes, with both showing maximum deviations of 10 kJ mol^{-1} or more, although they did offer considerable improvement over the corresponding straight DFT calculations. It would appear that the DFT methods examined have problems modeling the six-membered ring of the TEMPO species and, in a DFT-based ONIOM method, the ring would therefore have to be included in the core reaction.

Examining next the alkyl-halogen BDEs of the oligomeric halides (Table 6), we note that in this case also the low-cost methods fail to model the energetics of these reactions when compared with the high-level ab initio method G3(MP2)-RAD. Experimental values are only available for the two simplest reactions, the HP−Cl and HP−Br BDEs, and in those cases, G3(MP2)-RAD shows good agreement with experiment, well within the quoted experimental uncertainties. Using G3(MP2)-RAD as our benchmark, the MADs of RMP2, RHF, and the DFT methods typically exceed 10 kJ mol^{-1}, and in the small number of cases where they do not, the maximum deviations still exceed 17 kJ mol^{-1}. For the ONIOM calculations, we first note that in defining the core reaction, only α substituents were included with those beyond the α position being deleted. This resulted in an enormous saving in the computational cost. However, it should be noted that the α ester groups were included as intact substituents as they are effectively conjugated with the radical center. Defined in this way, the ONIOM technique led to greatly reduced errors. For example, the MAD for the B3LYP-ONIOM method is just 5 kJ mol^{-1} compared with 42.4 kJ mol^{-1} for the straight B3LYP calculations, that for BMK−ONIOM is only 2.9 kJ mol^{-1} compared with 7.7 kJ mol^{-1} for straight BMK calculations, and the RMP2-ONIOM method has an MAD of just 0.8 kJ mol^{-1}, much lower than that for the straight RMP2 calculations (27.6 kJ mol^{-1}). However, when the maximum errors are taken into account, it is again clear that only the RMP2-ONIOM technique (which has a maximum error of just 4.8 kJ mol^{-1}) is sufficiently accurate for quantitative purposes. As discussed elsewhere,[38] the mechanism by which the remote substituents affect the BDEs in these reactions is primarily steric in origin, assisted by

SCHEME 1: Addition, Ring-Opening, and Abstraction Reactions Studied in Table 7

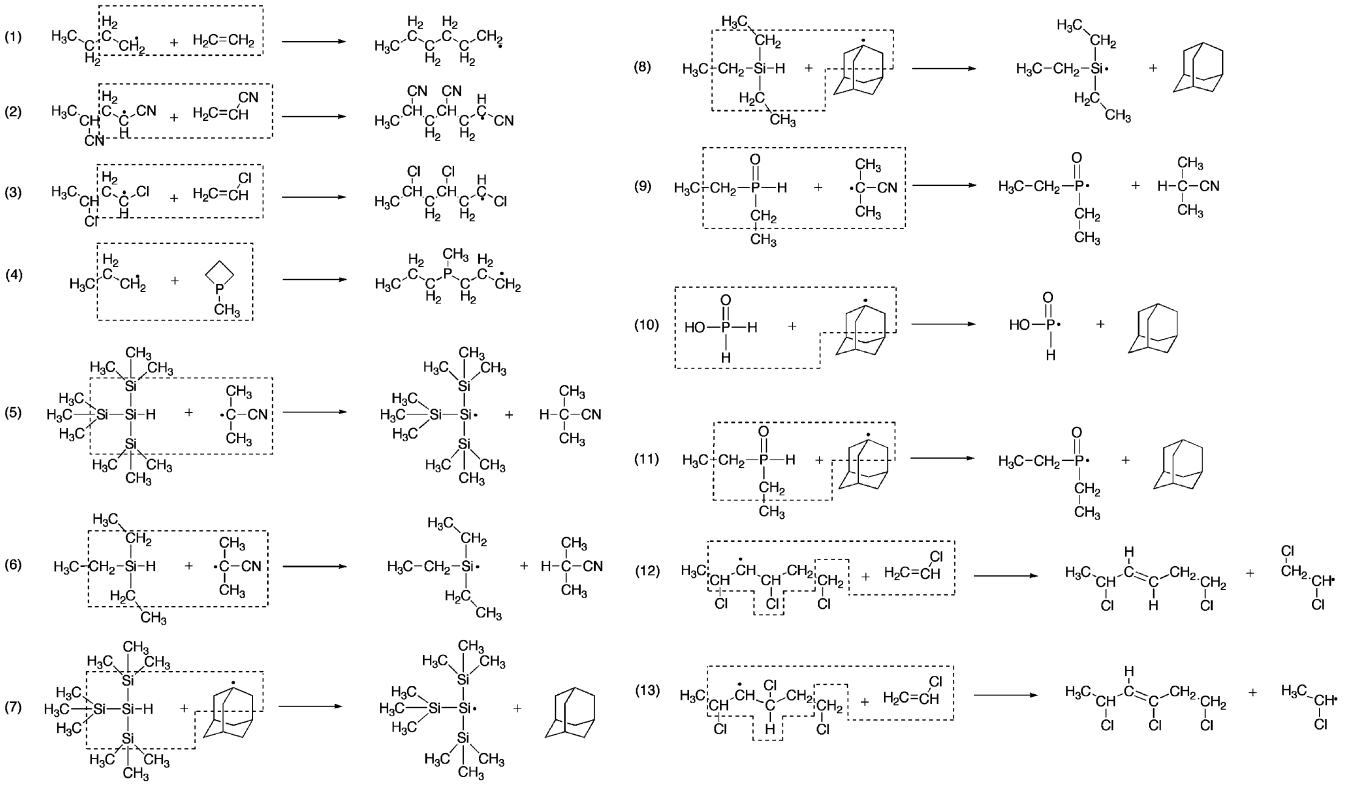

Dotted Line Indicates the Heavy Atoms Included in the Core Reaction in the ONIOM Calculations.

intramolecular hydrogen bonding. It therefore seems likely that the problem that these DFT methods have in measuring the remote substituent effects may be related to the more systemic problems that contemporary DFT methods show in measuring both medium- and long-range correlation effects.[5]

Finally, Table 7 shows the enthalpies of the 13 radical reactions shown in Scheme 1, covering radical addition, ring-opening, and various types of hydrogen and halogen transfer. The reactions predominantly involve carbon-centered radicals, although a limited number also involve silicon- and phosphorus-centered radicals. Where possible, experimental values of the reaction energies were calculated by using the relevant BDEs and/or heats of formation of the reactants and products.[31,32] Where comparison was possible, the agreement between G3-(MP2)-RAD and experiment was close to or within the quoted experimental uncertainties, particularly once the range of available experimental values for any individual species were taken into account. Using G3(MP2)-RAD as our benchmark, it is seen that the low-cost methods perform slightly better for these systems when compared with their performance for the various BDEs (e.g., Tables 5 and 6). This is not surprising, as one would expect a greater cancellation of error when the unpaired electron appears on both sides of the reaction. Nonetheless, all of the low-cost methods show maximum deviations of 15 kJ mol^{-1} or more and are therefore not sufficiently reliable for quantitative applications. In contrast,

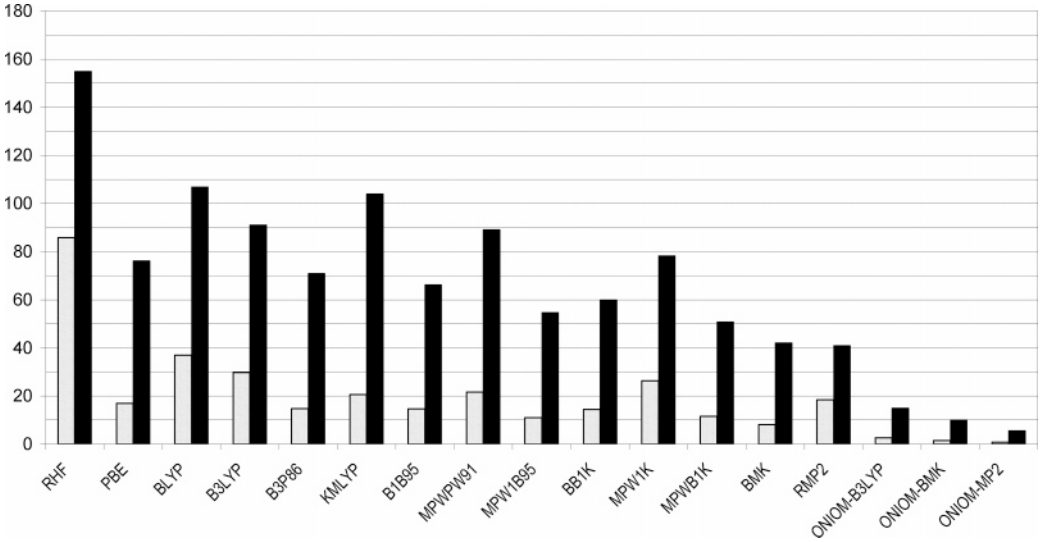

Figure 5. Overall mean □ and maximum ■ absolute deviations of the lower-cost computational methods from G3(MP2)-RAD for the 112 reactions in this study.

the ONIOM methods show greatly improved performance: all ONIOM methods have MADs of less than 4 kJ mol^{-1}, with the RMP2-ONIOM having the lowest MAD (1.2 kJ mol^{-1}). Both RMP2-ONIOM and BMK-ONIOM have maximum errors of 4.2 kJ mol^{-1} or less and would both be suitable for quantitative applications. However, in the light of their performance in the other case studies, only the RMP2-ONIOM method could be considered reliable enough for general use in radical thermochemistry, provided all α substituents are included in the core.

Conclusions

In the present work, we have shown that all of the DFT methods tested fail to provide an accurate description of the energetics of radical reactions when compared with G3(MP2)-RAD benchmark values, with even the best methods showing unpredictable deviations of more than 40 kJ mol^{-1} for some reactions (see Figure 5). The ab initio method RMP2 also shows large deviations for the absolute values the enthalpies of some types of reaction and, although it fares somewhat better than the DFT methods in modeling the relative values, it fails for substituents capable of strongly interacting with the unpaired electron. Fortunately, it is possible to obtain cost-effective accurate calculations for radical reactions using ONIOM-based procedures in which a high-level method such as G3(MP2)-RAD is only used to model the core reaction and the full system is modeled using a lower-cost procedure such as RMP2. Our present testing suggests that, provided the core reaction includes all substituents α to the reaction center and provided functional groups such as phenyl rings and ester linkages are treated as intact units, such a method is capable of modeling radical thermochemistry to within chemical accuracy (ca. 4 kJ mol^{-1}). Such an approach promises to extend the range of systems for which accurate computational thermochemistry is possible.

Acknowledgment. We gratefully acknowledge many useful discussions with Professor Peter Gill, generous allocations of computing time from the Australian Partnership for Advanced Computing and the Australian National University Supercomputing Facility, and support from the Australian Research Council under their Centres of Excellence program.

Supporting Information Available: B3LYP/6-31G(d) optimized geometries in the form of GAUSSIAN archive entries. This material is available free of charge via the Internet at http://pubs.acs.org.

References and Notes

(1) For recent successful applications in controlled radical polymerization, see for example: (a) Coote, M. L.; Henry, D. J. *Macromolecules* **2005**, *38*, 5774−5779. (b) Coote, M. L.; Izgorodina, E. I.; Krenske, E. H.; Busch, M.; Barner-Kowollik, C. *Macromol. Rapid Commun.* **2006**, *27*, 1015−1022. (c) Coote, M. L.; Krenske, E. H.; Izgorodina, E. I. *Macromol. Rapid Commun.* **2006**, *27*, 473−497 and references cited therein.

(2) Izgorodina, E. I.; Coote, M. L.; Radom, L. *J. Phys. Chem. A* **2005**, *109*, 7558−7566.

(3) Izgorodina, E. I.; Coote, M. L. *J. Phys. Chem. A* **2006**, *110*, 2486−2492.

(4) Izgorodina, E. I.; Coote, M. L. *Chem. Phys.* **2006**, *324*, 96−110.

(5) See for example: (a) Check, C. E.; Gilbert, T. M. *J. Org. Chem.* **2005**, *70*, 9828−9834. (b) Matsuda, S. P. T.; Wilson, W. K.; Xiong, Q. *Org. Biomol. Chem.* **2006**, *4*, 530−543. (c) Wodrich, M. D.; Corminboeuf, C.; Schleyer, P. v. R. *Org. Lett.* **2006**, *8*, 3631−3634. (d) Grimme, S. *Angew. Chem., Int. Ed.* **2006**, *45*, 4460−4464. (e) Wodrich, M. D.; Corminboeuf, C.; Schreiner, P. R.; Fokin, A. A.; Schleyer, P. v. R. *Org. Lett.* **2007**, *9*, 1851−1854. (e) Curtiss, L. A.; Raghavachari, K.; Redfern, P. C.; Pople, J. A. *J. Chem. Phys.* **2000**, *112*, 7374−7383.

(6) Frisch, M. J.; Trucks, G. W.; Schlegel, H. B.; Scuseria, G. E.; Robb, M. A.; Cheeseman, J. R.; Montgomery, J. A., Jr.; Vreven, T.; Kudin, K. N.; Burant, J. C.; Millam, J. M.; Iyengar, S. S.; Tomasi, J.; Barone, V.; Mennucci, B.; Cossi, M.; Scalmani, G.; Rega, N.; Petersson, G. A.; Nakatsuji, H.; Hada, M.; Ehara, M.; Toyota, K.; Fukuda, R.; Hasegawa, J.; Ishida, M.; Nakajima, T.; Honda, Y.; Kitao, O.; Nakai, H.; Klene, M.; Li, X.; Knox, J. E.; Hratchian, H. P.; Cross, J. B.; Bakken, V.; Adamo, C.; Jaramillo, J.; Gomperts, R.; Stratmann, R. E.; Yazyev, O.; Austin, A. J.; Cammi, R.; Pomelli, C.; Ochterski, J. W.; Ayala, P. Y.; Morokuma, K.; Voth, G. A.; Salvador, P.; Dannenberg, J. J.; Zakrzewski, V. G.; Dapprich, S.; Daniels, A. D.; Strain, M. C.; Farkas, O.; Malick, D. K.; Rabuck, A. D.; Raghavachari, K.; Foresman, J. B.; Ortiz, J. V.; Cui, Q.; Baboul, A. G.; Clifford, S.; Cioslowski, J.; Stefanov, B. B.; Liu, G.; Liashenko, A.; Piskorz, P.; Komaromi, I.; Martin, R. L.; Fox, D. J.; Keith, T.; Al-Laham, M. A.; Peng, C. Y.; Nanayakkara, A.; Challacombe, M.; Gill, P. M. W.; Johnson, B.; Chen, W.; Wong, M. W.; Gonzalez, C.; Pople, J. A. *Gaussian 03*, revision C.02; Gaussian, Inc.: Wallingford, CT, 2004.

(7) Amos, R. D.; Bernhardsson, A.; Berning, A.; Celani, P.; Cooper, D. L.; Deegan, M. J. O.; Dobbyn, A. J.; Eckert, F.; Hampel, C.; Hetzer, G.; Knowles, P. J.; Korona, T.; Lindh, R.; Lloyd, A. W.; McNicholas, S. J.; Manby, F. R.; Meyer, W.; Mura, M. E.; Nicklass, A.; Palmieri, P.; Pitzer, R.; Rauhut, G.; Schütz, M.; Schumann, U.; Stoll, H.; Stone, A. J.; Tarroni, R.; Throsteinsson, T.; Werner, H.-J. *MOLPRO 2002.6*, a package of ab initio programs; University of Birmingham: Birmingham, U.K., 2003.

(8) Scott, A. P.; Radom, L. *J. Phys. Chem.* **1996**, *100*, 16502−16513.

(9) Henry, D. J.; Sullivan, M. B.; Radom, L. *J. Chem. Phys.* **2003**, *118*, 4849−4860.

(10) A referee has subsequently alerted us to the publication of this basis set by the Curtiss group on the G3 website, http://chemistry.anl.gov/compmat/comptherm.htm.

(11) See for example: Wong, M. W.; Radom, L. *J. Phys. Chem.* **1998**, *102*, 2237−2245.

(12) See for example: Gómez-Balderas, R.; Coote, M. L.; Henry, D. J.; Radom, L. *J. Phys. Chem. A* **2004**, *108*, 2874−2883.

(13) Pople, J. A.; Gill, P. M. W.; Handy, N. C. *Int. J. Quantum Chem.* **1995**, *56*, 303−305.

(14) (a) Becke, A. D. *Phys. Rev. A* **1988**, *38*, 3098. (b) Lee, C.; Yang, W.; Parr, R. G. *Phys. Rev. B* **1988**, *37*, 785.

(15) Perdew, J. P.; Burke, K.; Ernzerhof, M. *Phys. Rev. Lett.* **1996**, *77*, 3865.

(16) Becke, A. D. *J. Chem. Phys.* **1993**, *98*, 5648.

(17) Perdew, J. P. *Phys. Rev. B* **1986**, *33*, 8822.

(18) Kang, J. K.; Musgrave, C. B. *J. Chem. Phys.* **2001**, *115*, 11040−11051.

(19) Zhao, Y.; Pu, J.; Lynch, B. J.; Truhlar, D. G. *Phys. Chem. Chem. Phys.* **2004**, *6*, 673−676.

(20) Adamo, C.; Barone, V. J. *J. Chem. Phys.* **1998**, *108*, 664−675.

(21) Zhao, Y.; Truhlar, D. G. *J. Phys. Chem. A* **2004**, *108*, 6908−6918.

(22) Zhao, Y.; Lynch, B. J.; Truhlar, D. G. *J. Phys. Chem. A* **2004**, *108*, 2715−2719.

(23) Lynch, B. J.; Fast, P. L.; Harris, M.; Truhlar, D. G. *J. Phys. Chem. A* **2000**, *104*, 4811−4815.

(24) Boese, A. D.; Martin, J. M. L. *J. Chem. Phys.* **2004**, *121*, 3405−3416

(25) It should be noted that, in applying the HLC, we interpreted the "number of lone pair electrons" to mean the total number of electrons in lone pairs. However, we noticed that the MAD of KMLYP versus experiment for the 34 reactions for which testing was possible improved from 13.0 to 5.7 kJ mol^{-1} if we treated n_p as the number of lone pairs and counted π bonds as lone pairs. These changes to the HLC would have improved the absolute values of the halide BDEs and the β-scission reactions but would not have affected the other BDEs or reaction energies. Moreover, because the HLC cancels entirely from the relative values of the reaction energies, the use of the improved HLC did not affect the main comparisons between KMLYP and G3(MP2)-RAD made throughout this study.

(26) Vreven, T.; Morokuma, K. *J. Comput. Chem.* **2000**, *21*, 1419−1432.

(27) Curtiss, L. A.; Raghavachari, K. *Theor. Chem. Acc.* **2002**, *108*, 61−70.

(28) Coote, M. L. *J. Phys. Chem. A* **2004**, *108*, 3865−3872.

(29) Coote, M. L.; Wood, G. P. F.; Radom, L. *J. Phys. Chem. A* **2002**, *106*, 12124−12138

(30) Toy, A. Ah.; Chaffey-Millar, H.; Davis, T. P.; Stenzel, M. H.; Izgorodina, E. I.; Coote, M. L.; Barner-Kowollik, C. *Chem. Commun.* **2006**, 835−837.

(31) Unless noted otherwise, experimental BDEs are taken from Luo, Y.-R. *Handbook of Bond Dissociation Energies in Organic Compounds*; CRC Press: Boca Raton, FL, 2003, and corrected to 0 K using calculated B3LYP/6−31G(d) temperature corrections. Where multiple experimental values are quoted, the value recommended by Luo is used.

(32) The heats of formation of the closed-shell species needed to calculate the experimental β-scission energies in Tables 2 and 7 were taken from the *NIST Chemisty WebBook*; NIST Standard Reference Database 69;

June 2005 release, *http://webbook.nist.gov/chemistry/*. Where multiple values are quoted, the most recent values were used.

(33) Coote, M. L.; Pross, A.; Radom, L. In *Fundamental World of Quantum Chemistry: A Tribute to the Memory of Per-Olov Löwdin, Volume III*; Brändas, E. J., Kryachko, E. J., Eds.; Kluwer-Springer: Dordrecht, The Netherlands, 2004; pp 563−579.

(34) Coote, M. L. *J. Phys. Chem. A* **2005**, *109*, 1230−1239.

(35) Note that these are the MADs for the relative values of ΔH (relative to $\Delta H = 0$ for R = CH_3), and not for the absolute enthalpies (as calculated in the original work). Normally one would expect smaller MADs in the relative values due to systematic cancellation of error. For RMP2, this is the case; however, with the DFT methods, the errors accumulate and the MADs are actually larger.

(36) Gill, P. M. W.; Pople, J. A.; Radom, L.; Nobes, R. H. *J. Chem. Phys.* **1988**, *89*, 7307−7314.

(37) (a) Zhao, Y.; Schultz, N. E.; Truhlar, D. G. *J. Chem. Theory Comput.* **2006**, *2*, 364−382. (b) Zhao, Y.; Truhlar, D. G. *Org. Lett.* **2006**, *8*, 5753−5755.

(38) Lin, C. Y.; Coote, M. L.; Petit, A.; Richard, P.; Poli, R.; Matyjaszewski, K. *Macromolecules* **2007**, 40, 5985−5994.

(39) Longshaw, A. I.; Carland, M.; Krenske, E.; Coote, M. L.; Sherburn, M. S. *Tetrahedron Lett.* **2007**, *48*, 5585−5588